

**THE INFLUENCE OF GRAVITY ON
 $Pb_{1-x}Sn_xTe$ CRYSTALS GROWN BY
THE VERTICAL BRIDGMAN METHOD**

Y.A. Chen,¹ I.N. Bandeira,¹ A.H. Franzan,¹ S. Eleutério Filho,²
and M.R. Slomka²

¹Laboratório Associado de Sensores e Materiais - LAS
Instituto de Pesquisas Espaciais - INPE
São José dos Campos, SP 12201, Brazil

²Centro Tecnológico de Informatica - CTI
Campinas, SP 13093, Brazil

ABSTRACT

Composition profiles of $Pb_{0.80}Sn_{0.20}Te$ grown by the normal and inverted Bridgman methods are presented. The growth under stabilized solute gradient decreases the convection, and the final solute distribution corresponds to the partial diffusion-convective mechanism. Also shown are results of high-gravity gradient freeze growth with a destabilizing temperature gradient.

INTRODUCTION

The inverted vertical Bridgman method (IVB), where the solidification occurs from the top of the melt under a destabilizing thermal gradient, allows growth of crystals with buoyancy-driven convection different from that with the usual vertical Bridgman configuration (VB). Due to the unstable solutal gradient, the compositional profile of $Pb_{0.80}Sn_{0.20}Te$ crystals grown by VB usually obeys the normal freezing law. It is well known that for Bridgman growth in a microgravity environment, the convection is suppressed, and a crystal with homogeneous composition can be grown with a diffusion-controlled steady state. However, experiments in space are restricted by technical and financial constraints, and alternatives, such as the IVB or growth under high gravity using centrifugal systems,¹⁻³ are becoming useful techniques to study the influence of gravity on crystallization processes.

Only a few materials have been grown by IVB.⁴⁻⁷ Recently the pseudobinary compound

$\text{Pb}_{1-x}\text{Sn}_x\text{Te}$ has also been investigated.^{8,9} This paper reports the influence of convection on the longitudinal composition profile in $\text{Pb}_{0.80}\text{Sn}_{0.20}\text{Te}$ crystals grown by VB and IVB at earth's gravity (1 g) and by the inverted gradient freeze technique at 3 g.

EXPERIMENTAL

The experimental system for inverted gradient freeze growth at 3 g is shown in Fig. 1. For all experiments the growth ampoule consists of a quartz rod of 8 mm diameter and 20 mm length with a $\text{Pb}_{0.80}\text{Sn}_{0.20}\text{Te}$ charge (8 mm diameter, 40 mm length, 69 purity) sealed in an evacuated (10^{-6} Torr) quartz ampoule with approximately the same internal diameter. This ampoule (~ 100 mm total length, 1.5 mm thickness) has a constriction (~ 10 mm length, ~ 3 mm diameter) for seed selection. Enough charge powder is added to fill all empty spaces after melting. The quartz rod placed on top of the melt avoids material loss by evaporation. The quartz ampoule is sealed inside a steel cartridge.

For the VB and IVB experiments at 1 g, the cartridge containing the ampoule was placed in a vertical furnace with 80 cm length and 3.5 cm internal diameter. The furnace was heated to 950 °C, yielding a temperature gradient G of 16 °C/cm along the cartridge at the estimated position of the solid-liquid interface. Growth was caused by moving the

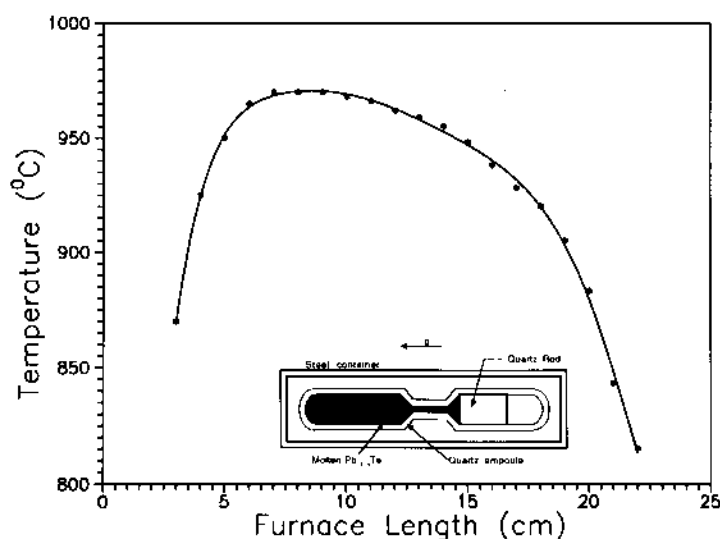


Figure 1. Temperature profile and ampoule arrangement for an inverted gradient freeze experiment at 3 g. The temperature profile was measured along the steel container.

ampoule through the furnace at $V=1.35$ mm/hr. For VB growth the ampoule was lowered by means of a stepping motor. For IVB growth the furnace was turned over and the ampoule slowly raised for growth.

The growth under high gravity was carried out in a smaller furnace (30 cm length and 2 cm internal diameter), which was attached to a centrifuge (maximum radius = 1 m) built at INPE. This centrifuge gives a resulting acceleration up to 10 g. After heating and

stabilization, the centrifuge was accelerated to the desired level, and the growth was carried out by slowly lowering the furnace temperature. The growth conditions were approximately the same as at 1 g.

The SnTe axial concentration was measured through an Electron Probe Microanalyzer. The conversion from X-ray intensity to solute concentration was based on a calibration curve obtained from standard samples with known composition.

RESULTS AND DISCUSSION

During growth by VB the gravitational vector and temperature gradient are antiparallel. The solute SnTe is rejected from the solid-liquid interface, forming a piled-up layer on the liquid side. This accumulated layer with a less dense component is reduced by convective flows in the melt, and usually the composition of the growing material follows the normal distribution. Figure 2 shows the experimental compositions as points. The lines are third-order polynomial fits to the experimental data for mole fraction SnTe.

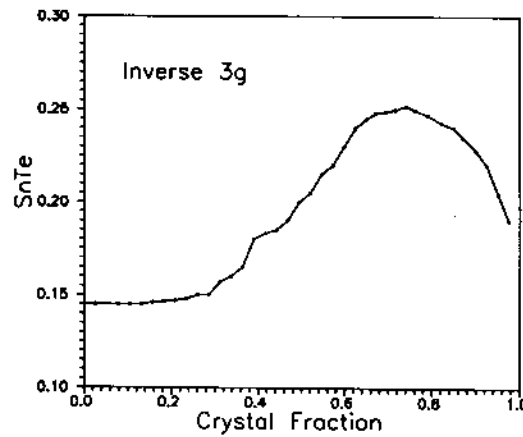


Figure 2. Solute distribution along the axial direction for crystals grown by the usual and inverted vertical Bridgman methods at 1 g.

In order to evaluate the influence of both solutal and thermal gradients on convection, their corresponding values of density gradient are compared. The density gradient caused by solute accumulation at the interface is given by:¹⁰

$$\left(\frac{\partial \rho}{\partial Z} \right)_c = \frac{\partial \rho}{\partial C} \frac{\partial C}{\partial Z} = \frac{\partial \rho}{\partial C} \left(\frac{1}{k_0} - 1 \right) \frac{V C_0}{D} \quad (1)$$

at steady state. The density gradient due to the temperature gradient is:

$$\left(\frac{\partial \rho}{\partial Z} \right)_T = \frac{\partial \rho}{\partial T} \frac{\partial T}{\partial Z} = \frac{\partial \rho}{\partial T} G \quad (2)$$

Here $k_0 = 0.61$, $V = 1.35$ mm/h, $C_0 = 0.20$, $D = 5.3 \times 10^{-5}$ cm²/s, and $G = 16$ °C/cm are equilibrium segregation coefficient, solidification rate, original mole fraction of SnTe, diffusion coefficient in the melt, and temperature gradient, respectively. The values $\partial\rho/\partial C = 1.62$ g/cm³.mol and $\partial\rho/\partial T = 8.3 \times 10^{-4}$ g/cm³.°C are calculated from coefficients of bulk solutal and thermal expansion. Using these parameters, the numerical values of Eq. (1) and Eq. (2) are 1.46×10^{-1} g/cm⁴ and 1.33×10^{-2} g/cm⁴, respectively. The solutal density gradient is about ten times bigger than the thermal density gradient at the interface. This might explain the strong convective behavior presented in VB, and also the reduced convection during IVB growth (Fig. 2). However, since the solute concentration decreases exponentially into the liquid, it is likely that away from the interface, the temperature gradient becomes the dominant term. A complex compositional layering may occur in the melt.¹¹

According to the results for IVB, the composition profile (Fig. 2) corresponds to partial melt mixing, where the convection flow is sufficiently weak to allow the formation of a solute boundary layer. Solutal convection is suppressed, because of the stable density gradient [Eq. (1)], and hence the diffusion-controlled solidification is not interrupted.

Convection is a function of the thermal Rayleigh number Ra_T , the solutal Rayleigh number Ra_S , the thermal Grashof number Gr_T , and the solutal Grashof number Gr_S . The definitions for Ra and Gr are:

$$Ra_s = \frac{\beta_s}{D\nu} gh^4 \frac{\partial C}{\partial z} \quad Ra_T = \frac{\beta_T}{\alpha\nu} gh^4 \frac{\partial T}{\partial z}$$

$$Gr_s = g\beta_s h^3 \Delta C / \nu^2 \quad Gr_T = g\beta_T h^3 \Delta T / \nu^2$$

where β is the coefficient of bulk solutal or thermal expansion, D is the diffusion coefficient in the melt, ν is the kinematic viscosity, α is the thermal diffusivity and h is the

Table 1. Rayleigh and Grashof numbers for $Pb_{0.80}Sn_{0.20}Te$.

h/ϕ	$h(\text{cm})$	Ra_T	Ra_S	Gr_T	Gr_S	$\delta(\text{cm})$
0.625	0.5	2×10^3	5×10^6	2×10^4	2×10^5	3×10^{-2}
1.200	1.0	4×10^4	7×10^7	2×10^5	3×10^6	2×10^{-2}
2.000	2.0	6×10^5	1×10^9	6×10^6	4×10^7	1×10^{-2}
3.750	3.0	3×10^6	6×10^9	2×10^7	2×10^8	7×10^{-3}
5.000	4.0	1×10^7	2×10^{10}	6×10^7	7×10^8	5×10^{-3}

liquid height. Estimated values for our IVB experiments are shown in Table 1 for an ampoule diameter ϕ of 8 mm.

According to previous experiments,⁸ the critical thermal Rayleigh number is 2×10^3 for an aspect ratio of 0.270, confirming that IVB was grown in the presence of some convection. The thickness of the solutal stagnant film δ can be estimated from a correlation for vertical zone melting of naphthalene:¹²

$$\delta = \frac{10r}{B(r/h)^{0.44} (hV/D)^{0.26}} \quad (3)$$

where $r = \phi/2$ is the ampoule radius, h is the height of the molten zone, and:

$$B = (Pr)^{-1/4} (Sc)^{1/2} [Gr_T + (Pr/Sc)^{1/2} Gr_S]^{1/4} \quad (4)$$

where $Pr = 2 \times 10^3$ (Prandtl) and $Sc = 53$ (Schmidt). Calculated values of δ are shown in Table 1. These yield estimates for $\delta V/D$ ranging from 0.004 to 0.02. Since $\delta V/D \ll 1$, the above correlation predicts complete mixing. This does not correspond to our experimental results. It should also be noted that the diffusional solute layer thickness D/V is approximately 13 mm.

The solute composition profile for inverted gradient freeze growth is shown in Fig. 3. This complex behavior is indicative of dramatic changes in convection or freezing rate as solidification proceeds.

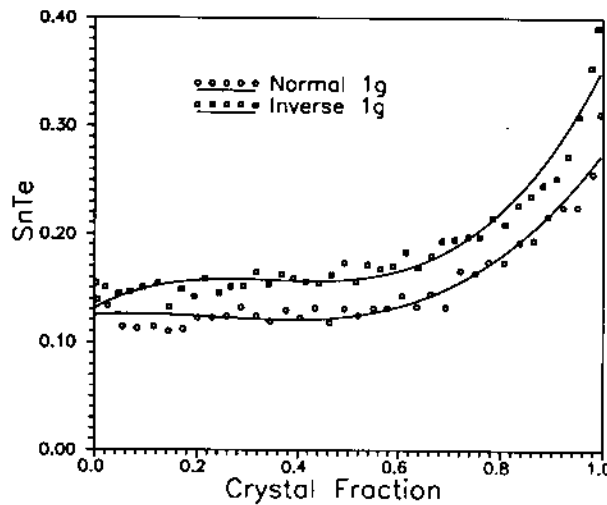


Figure 3. Solute distribution along axial direction for inverted gradient freeze growth at 3 g.

CONCLUSIONS

The inverted Bridgman method allows the growth of $Pb_{0.80}Sn_{0.20}Te$ crystals with a stabilizing solute gradient. Due to a reduction in convection, the final composition profile is similar to that provided by a partial diffusive mechanism. Inverted gradient freeze growth under high gravity yields a concentration profile indicating dramatic variation in convection or freezing rate during the solidification.

REFERENCES

1. G. Müller, E. Schmidt, and P. Kyr, *J. Cryst. Growth* 49:387 (1980).
2. H. Rodot, L.L. Regel, and A.M. Turtchaninov, *J. Cryst. Growth* 104:280 (1990).
3. L.L. Regel, A.M. Turtchaninov, O.V. Shumaev, I.N. Bandeira, Y.A. Chen, and P.H.O. Rappl, *J. Cryst. Growth* 119:94 (1992).
4. W.J. Boettinger, S.R. Coriell, F.S. Biancanello, and M.R. Cordes. "NBS: Materials Measurements" (NBSIR 80-2082), Annual Report (July 1980).
5. G. Müller, G. Neumann, and W. Weber, *J. Cryst. Growth* 70:78 (1984).
6. K.M. Kim, A.F. Witt, and H.C. Gatos, *J. Electrochem. Soc.* 119:1218 (1972).
7. H. Jamgotchian, B. Billa, and L. Capella, *J. Cryst. Growth* 85:318 (1987).
8. K. Graszka and A. Jedrzejczak, *J. Cryst. Growth* 110:867 (1991).
9. K. Graszka and U. Zuzga-Graszka, *J. Cryst. Growth* 116:139 (1992).
10. R.M. Sharp and A. Hellawell, *J. Cryst. Growth* 12:261 (1972).
11. D.T.J. Hurle, G. Müller, and R. Nitsche, Fluid sciences and materials science in space, H.U. Walter, ed., European Space Agency, Springer-Verlag (1987).
12. W.R. Wilcox, Mass transfer in fractional solidification, in: "Fractional Solidification," M.Zief and W.R. Wilcox, eds., Dekker, N.Y. (1967) p. 61,62.
13. V. Fano, R. Pergolari, and L. Zanotti, *J. Mater. Sci.* 14:535 (1979).